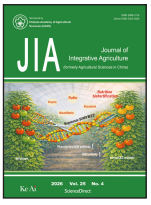
*Journal of Integrative Agriculture 2026, 25(4): 1716–1730*

Available online at ScienceDirect

Journal of Integrative Agriculture



RESEARCH ARTICLE

# Monitoring of agricultural drought based on multi-source remote sensing data in Heilongjiang Province, China

**Chenfa Jiang[1, 2*], Changhui Ma[1*], Sibo Duan[1#], Xiaoxiao Min[1], Youzhi Zhang[3], Dandan Li[1], Xia Zhang[2]**

[1] *State Key Laboratory of Efficient Utilization of Arable Land in China/Institute of Agricultural Resources and Regional Planning, Chinese Academy of Agricultural Sciences, Beijing 100081, China*
[2] *Hebei International Joint Research Center for Remote Sensing of Agricultural Drought Monitoring, Hebei GEO University, Shijiazhuang 050031, China*
[3] *Institute of Agricultural Remote Sensing and Information, Heilongjiang Academy of Agricultural Sciences, Harbin 150086, China*

**Highlights**

- The multivariable linear regression was used to establish composite drought indices.
- MCDI-9 can effectively represent the affected area of drought, while MCDI-12 can effectively represent grain crop yields.
- Significant spatial variations in agricultural drought were observed throughout the region.
- Spring and early summer are the most drought-prone periods.

**Abstract**

Agriculture is the foundation of socio-economic development and is highly influenced by weather and climate conditions. Drought is one of the most significant threats to agricultural development and food security. Currently, *in-situ* drought monitoring based on weather stations and based on remote sensing data has limitations, including infrequent updates, limited coverage, and low accuracy. This study leverages multi-source remote sensing data to monitor agricultural drought in Heilongjiang Province, China. We developed multi-source composite drought indices (MCDIs) at various timescales (3, 6, 9, and 12 months) by integrating precipitation, land surface temperature, soil moisture, and vegetation indices. Utilizing remote sensing data from various sources, we calculated a series of single drought indices, which are the precipitation condition index, soil moisture condition index, vegetation condition index, and temperature condition index. These are then integrated into MCDIs using a multivariable linear regression approach. The analysis reveals that MCDIs correlate more with standardized precipitation evapotranspiration index (SPEI) than single drought indices. When examining the correlation between different MCDIs and the affected area of crops and major grain production, MCDI-9 showed the highest correlation with the affected area of crops, while MCDI-12 showed the highest correlation with grain production. This suggests that these two MCDIs at different timescales are better indicators of agricultural drought. The spatio-temporal analysis of MCDI indicates that drought in Heilongjiang Province primarily occurs in early spring, gradually spreading from the Greater Khingan Mountains region to the southeastern plains. The drought gradually alleviates during the summer, ending by the autumn harvest period. Therefore, the MCDIs constructed in this study can serve as effective methods and indicators for drought monitoring in Heilongjiang Province and similar regions.

**Keywords:** agricultural drought, spatio-temporal monitoring, multi-source remote sensing data, SPEI, Heilongjiang Province

## 1. Introduction

Drought is a natural phenomenon that occurs on multiple time scales and has a significant impact on the hydrological cycle across vast regions. As a frequent extreme occurrence, it poses significant threats to agricultural production and society (Wu *et al.* 2018; Haile *et al.* 2020; Mishra *et al.* 2021). Rising global temperatures have resulted in more frequent and widespread droughts in recent years, significantly impacting the vast semi-arid regions of the Northern Hemisphere (Wagner *et al.* 1999; Wang *et al.* 2015; Prăvălie 2016;

Received 18 February 2025; Received in revised form 2 March 2025; Accepted 20 March 2025; Available online 18 April 2025
Chenfa Jiang, E-mail: 22120405011@hgu.edu.cn; Changhui Ma, E-mail: machanghui@caas.cn; #Correspondence Sibo Duan, E-mail: duansibo@caas.cn
*These authors contributed equally to this study.

© 2026 CAAS. Publishing services by Elsevier B.V. on behalf of KeAi Communications Co. Ltd. This is an open access article under the CC BY-NC-ND license (http://creativecommons.org/licenses/by-nc-nd/4.0/). Peer review under responsibility of Editorial Board of *Journal of Integrative Agriculture*.
doi: 10.1016/j.jia.2025.04.027

Vicente-Serrano *et al.* 2020). Drought usually consists of four types: meteorological drought, agricultural drought, hydrological drought, and socio-economic drought (Wilhite and Glantz 1985; Saha *et al.* 2023). Over the past few decades, climate change has caused substantial changes in drought characteristics, notably increasing their severity, intensity, and duration, particularly in dryland regions (El-Beltagy *et al.* 2012; Liu and Hwang 2015; Ahmed *et al.* 2019). Dryland areas, which host about 43% of the world's croplands, are exceptionally vulnerable to variations in water availability (Michael *et al.* 2018; Koutroulis 2019). As a result, gaining a deeper understanding of drought dynamics in these regions is vital for enhancing water resource management and devising effective drought response and adaptation strategies (Meyer 1992; Vicente-Serrano *et al.* 2012; Vogt and Somma 2013; Kahil *et al.* 2015; Kuwayama *et al.* 2019; Zia *et al.* 2021).

Several *in-situ* drought indices, including the moisture index (MI) (Thornthwaite 1955), Palmer drought severity index (PDSI) (Palmer 1965), standardized precipitation index (SPI) (McKee *et al.* 1993), and standardized precipitation evapotranspiration index (SPEI) (Vicente-Serrano *et al.* 2010), are effective tools for monitoring drought conditions. The MI is commonly used to assess climate conditions related to dryness and wetness (Willmott and Feddema 1992). However, the MI has notable drawbacks, particularly its inability to account for spatial variations since it is typically based on point or regional averages, which may not accurately capture small-scale differences in dry and wet conditions. The PDSI is a useful metric for assessing the severity of long-term droughts at particular locations and times, though it is less effective for addressing short-term drought events and may produce varying results across different climatic regions (Zargar *et al.* 2011; Zhao *et al.* 2017). To overcome these limitations, the SPEI was introduced, offering greater versatility and applicability across various climates, making it more suitable for drought monitoring than the PDSI (Bezdan *et al.* 2019). However, since drought is a localized event, it must be monitored not only at specific sites but also across larger spatial scales. The spatial resolution of *in-situ* drought indices is dependent on the density and distribution of the site network (Kogan 1997; Kustas *et al.* 2011; Mukhawana *et al.* 2023). Remote sensing data offers systematic and continuous insights into vegetation and water cycles, enabling satellite-based drought indices to surpass the limitations of *in-situ* indices and be utilized for monitoring drought over larger spatial scales (Xu *et al.* 2018).

The normalized difference vegetation index (NDVI) is a widely utilized remote sensing tool for monitoring regional vegetation growth, which is closely associated with drought conditions. Various drought metrics have been derived from the NDVI, such as the anomaly vegetation index (Chen *et al.* 1994) and the vegetation condition index (VCI) (Kogan 1995a, b; Kogan 2007). NDVI-based drought indices are effective in reflecting reductions in leaf area and chlorophyll content in plants impacted by drought. Additionally, precipitation-based indices like the precipitation condition index (PCI), soil moisture-based indices such as the soil moisture condition index (SMCI), and indices derived from land surface temperature (LST), such as the temperature condition index (TCI) are also valuable for tracking the duration and effects of drought (Kogan 1995a; Rhee *et al.* 2010; Zhang and Jia 2013).

Given the diverse causes of drought, various composite drought indices have been developed by integrating individual drought indices derived from remote sensing such as the TCI, SMCI, PCI, and VCI, offering a more thorough approach to monitoring drought conditions. For instance, Rhee *et al.* (2010) developed the scaled drought condition index, which integrates the TCI, VCI, and PCI with varying weightings to track agricultural drought conditions in North and South Carolina, USA. The microwave-integrated drought index, which combines microwave indices derived from multiple sensors such as the SMCI, TCI, and PCI, is intended to identify short-term, particularly meteorological, drought distribution in North China (Zhang and Jia 2013). In addition, various other composite drought indices have been proposed, including the synthesized drought index (Du *et al.* 2013), the optimized vegetation drought index (Hao *et al.* 2015), the multivariate drought index (Waseem *et al.* 2015), and the process-based accumulated drought index (Zhang *et al.* 2017) are among the combined drought indices that have generally fulfilled researchers' expectations. However, the effectiveness of monitoring drought can differ by region, and many of these indices may fall short in accurately reflecting the impact of individual variables on drought development.

In particular, the modified drought severity index (MDSI) and the normalized standardized precipitation evapotranspiration index (NSPEI) have been proposed to address these issues by integrating both meteorological data and soil moisture. The MDSI, for example, combines soil moisture and evapotranspiration data to enhance agricultural drought monitoring, but its application is limited by station-based data, which restricts its regional applicability (Sun *et al.* 2022). On the other hand, NSPEI normalizes the SPEI, offering a more robust drought measure across diverse climatic zones, although it does not directly incorporate vegetation conditions or temperature data, which are critical for assessing drought impacts on agriculture (Vicente-Serrano *et al.* 2020). These indices complement traditional approaches but still face challenges in accurately capturing the multifaceted nature of drought, particularly in regions like Northeast China, where both precipitation and temperature anomalies interact complexly with soil moisture and vegetation health.

Compared to these existing methods, this study introduces the multi-source composite drought index (MCDI), which integrates precipitation, soil moisture, vegetation indices, and LST to offer a more comprehensive and flexible drought monitoring tool, with the added advantage of multi-timescale analysis. The term MCDI will be used consistently throughout this manuscript to refer to the composite index derived from these variables.

In this study, we employed the multivariable linear regression approach to develop MCDIs by consolidating data on precipitation, soil moisture, vegetation, and LST data to evaluate drought conditions in Heilongjiang Province,

China. The main objectives of this study are: 1) to establish MCDIs on 3-, 6-, 9-, and 12-month SPEI and compare the performance of composite indices versus single remote sensing indices in representing SPEIs; 2) to assess the effectiveness of MCDIs in monitoring agricultural drought; and 3) to examine drought conditions in Heilongjiang Province over spatial and temporal dimensions using MCDIs.

## 2. Materials and methods

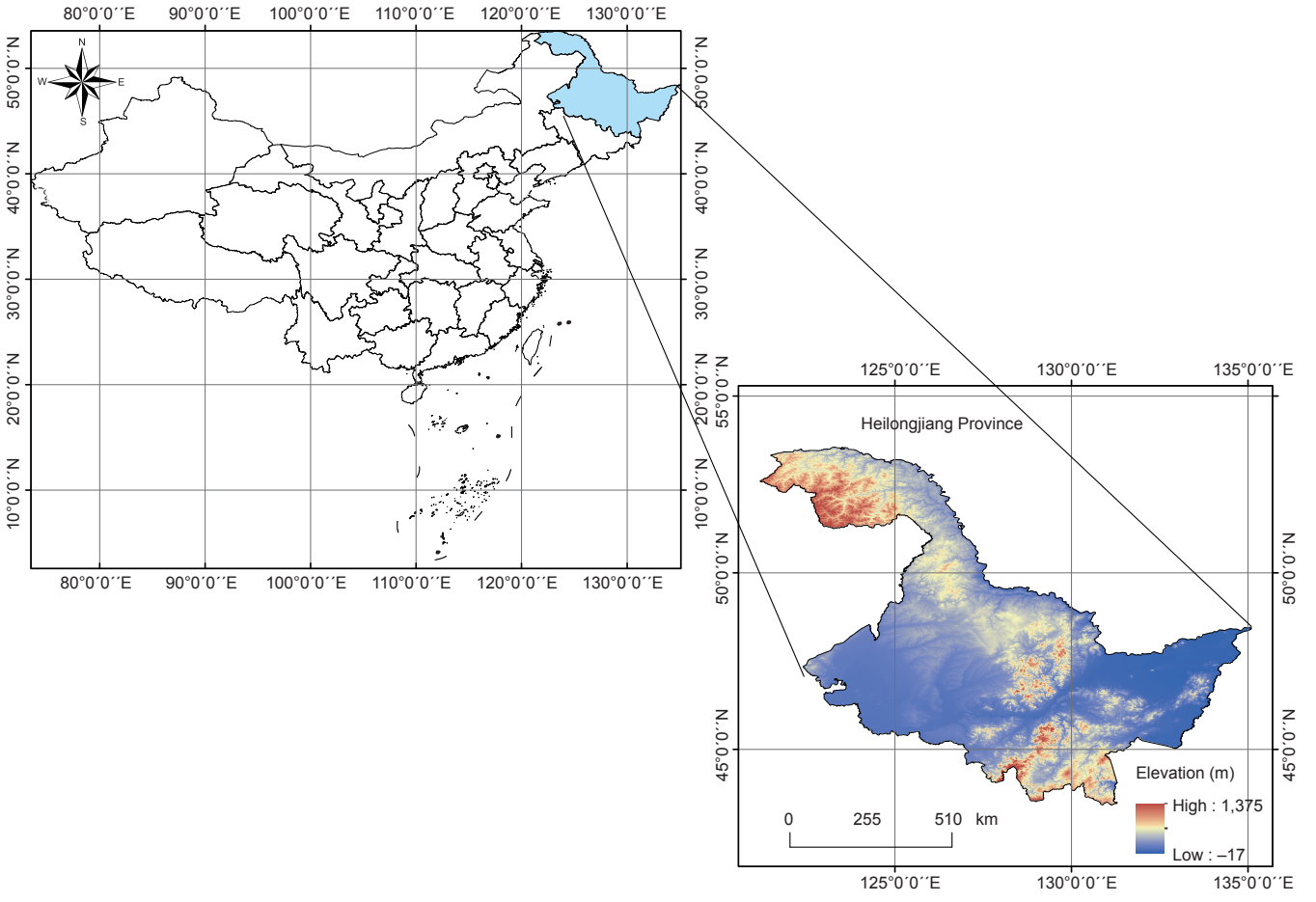
### 2.1. Study area

Heilongjiang Province is located in the northeastern part of China and is the northernmost province in the country (Fig. 1). The topography rises in the west and gradually falls towards the east, mountains are mainly distributed in the northwest, north, and southeast, and plains in the southwest and northeast. The terrain primarily consists of mountains, plateaus, and plains. Heilongjiang boasts abundant land and water resources, with the largest total cultivated land area in the country, and per capita cultivated land area is about four times the national average. The province's reserve cultivated land resources account for approximately 20% of the national total.

The climate in Heilongjiang is classified as temperate and cold temperate continental monsoon, characterized by significant diurnal temperature variations and distinct seasons. The province is divided into mid-temperate and cold temperate zones based on temperature and into humid, semi-humid, and semi-arid regions based on precipitation. Summers are marked by concurrent heat and rainfall, with average annual temperatures ranging from –5°C to 5°C, increasing from north to south, and annual precipitation between 400 and 650 mm (Li *et al.* 2024). The study area experiences its peak precipitation during the summer months, particularly from June to August, with the majority of rainfall occurring during the crop-growing season (March–October). Most of the precipitation occurs during the crop growth period, making the region suitable for planting single-crop annuals.

Agricultural land in Heilongjiang Province is predominantly located in the Songnen Plain (SNP) and the Sanjiang Plain (SJP). The SNP, situated in the southwestern part of the province and part of the larger Songliao Plain, spans 34 counties. This region, characterized by its soda-saline soils, is one of the three major global areas with such soil types (Zhou *et al.* 2019). In contrast, the SJP, which includes 23 counties in northeastern Heilongjiang, has many national-level wetland conservation areas (Dan *et al.* 2015). The SJP is rich in soil and water resources, establishing it as a key national rice production base.

Heilongjiang Province frequently experiences climate-related disasters. Data on agricultural disaster areas from




审图号 : GS 京 (2025) 2497 号

**Fig. 1 Location of the study area.**

1986 to 2021 show that the proportion of drought-affected areas has been relatively high since 2000. The years 2001, 2007, and 2009 were particularly severe, with drought-affected areas reaching 3.75 million, 6.5 million, and 4.87 million ha, respectively. Drought has a significant impact on agricultural production in Heilongjiang, with an average annual affected area of 1.53 million ha, underscoring drought as one of the major natural disasters affecting agriculture in the province.

### 2.2. Datasets

**Meteorological data** The monthly data, including cumulative precipitation, average temperature, 2-m wind speed, latitude, actual vapor pressure, sunshine duration, saturated vapor pressure, and relative humidity were obtained from the China Meteorological Data Service (http://data.cma.gov.cn) over the study area from 1986 to 2021. There are 13 weather stations with complete data records in the Heilongjiang Province.

Gridded precipitation data for the region were obtained from a 1-km resolution monthly dataset for China (Peng *et al.* 2017), which is freely available through the National Tibetan Plateau/Third Pole Environment Data Center (http://data.tpdc.ac.cn). This dataset provides spatially continuous precipitation estimates and complements station-based precipitation observations by offering high-resolution coverage across the study area. It was created using delta spatial downscaling from a global climatology dataset and was validated against data from 496 weather stations across China. In this study, gridded precipitation data were used for drought index calculations, whereas station-based precipitation data from meteorological stations were primarily utilized for validation and bias correction. However, the spatial resolution of these meteorological variables may differ from the 1-km precipitation data. To address this, *in-situ* meteorological station data were interpolated using the Inverse Distance Weighting method to generate gridded datasets with a 1-km resolution, ensuring consistency across all variables used for drought index calculations. The selection of the 1986–2021 time period for meteorological data was based on the requirement for calculating the SPEI. The SPEI is a standardized drought index that relies on historical precipitation and evapotranspiration data to define drought conditions relative to the long-term climate. According to the World Meteorological Organization (WMO) guidelines, a minimum of 30 years of continuous climate records is required to establish a reliable statistical baseline for indices like SPI and SPEI. Using a shorter time series would reduce the robustness of the probability distribution fitting, leading to less reliable drought classification.

Precipitation is the primary driver of drought conditions, and the PCI quantifies the deviation of precipitation from the long-term mean (Ezenwaji *et al.* 2017). It is particularly effective in detecting meteorological droughts, which typically precede agricultural and hydrological droughts.

**Soil moisture data** The soil moisture data used in this study is the Volumetric Soil Water Layer 1 (VSWL1) from the ERA5-Land dataset (https://cds.climate.copernicus.eu/). This data represents the water volume in the top soil layer (0–7 cm, with the soil surface as 0 cm). This dataset has a spatial resolution of 0.1° and a temporal resolution of 1 month, and it is widely used in numerous studies (Sabater 2019; Jiang *et al.* 2021; Bhardwaj *et al.* 2022). The spatial resolution of ERA5-Land data (0.1°) differs from the 1-km resolution of other remotely sensed data used in this study. To ensure consistency in spatial resolution, the ERA5-Land soil moisture data were bilinearly interpolated to a 1-km grid, aligning it with the other data layers used for drought index calculations. This interpolation method is commonly used in hydrological studies to improve spatial consistency across datasets. Soil moisture data from the ERA5-Land dataset, covering the period from 2017 to 2021, were used to analyze drought conditions.

Soil moisture is a crucial factor in agricultural drought assessment, as it directly affects crop water availability(Souza *et al.* 2021). SMCI has been widely applied in drought monitoring due to its ability to reflect short-term soil moisture fluctuations, especially in rainfed agricultural regions.

**Remote sensing data** Monthly VCI and TCI were derived from MODIS NDVI and LST data for the period from March to September each year between 2017 and 2021. The LST (1-day, MOD11A1, Collection v006) and NDVI (30-day, MOD13A3, Collection v006) data, both with a 1 km resolution, were obtained from NASA's Earth Observing System Data and Information System (EOSDIS) (http://reverb.echo.nasa.gov). The selection of the 2017–2021 period for VCI and TCI data was based on its role in constructing and fitting the MCDI. This period was chosen to ensure consistency with other high-resolution datasets while capturing recent drought variability for model calibration. The MCDI model was trained using these years to establish robust relationships between remote sensing drought indices and meteorological drought indicators, facilitating accurate drought monitoring and assessment.

The VCI is derived from NDVI and indicates vegetation health, making it suitable for assessing agricultural and ecological droughts (Kogan 2007). It is particularly useful in regions where soil moisture availability significantly impacts crop growth and productivity. High temperatures exacerbate drought severity by increasing evapotranspiration and reducing soil moisture retention. TCI, derived from LST, provides insights into drought-induced heat stress on vegetation (Mishra and Singh 2010).

**Statistical data** In this study, crop yield and the extent of crop area affected by drought were used as proxy variables to represent the severity of agricultural drought conditions, showing how drought adversely affects crop growth and productivity. The data on the agricultural land area affected by drought in Heilongjiang Province from 1986 to 2021 and the data on different grain yields from 2000 to 2021 were sourced from the *China Rural Statistical Yearbook* (https://www.stats.gov.cn/) and *China Water and Drought Disaster Defense Bulletin* (http://mwr.gov.cn/zzsc/).

Different datasets were resampled to a common spatial resolution of 1 km to facilitate intercomparisons and improve consistency in analysis. Specifically, precipitation data from the 1-km gridded dataset was directly used, while station-based meteorological variables (e.g., temperature, wind speed, humidity) were interpolated using the Inverse

Distance Weighting method. Soil moisture data from ERA5-Land, originally at a spatial resolution of 0.1° (~9–11 km), was downscaled to 1 km using bilinear interpolation. The MODIS-derived vegetation and land surface temperature indices (VCI and TCI) were already at a 1-km resolution and required no further resampling. Once the data were acquired and processed, we applied the linear regression model for drought index calculation, as described in the following section.

### 2.3. Single drought index

In this study, we use the precipitation dataset to calculate the monthly PCI in Heilongjiang Province. After obtaining the precipitation data, the next step is to compute the PCI based on these monthly precipitation values. The formula is as follows:

$$\mathrm{PCI}=\frac{Tp_i-Tp_{\min}}{Tp_{\max}-Tp_{\min}} \quad (1)$$

where $Tp_{max}$ and $Tp_{min}$ refer to the historically highest and lowest precipitation values at each specified time step throughout the study period, and $Tp_i$ indicates the precipitation for the $i$ month (Zhang and Jia 2013), $i$ is a time step representing a specific month.

The soil mositure (SM) data were resampled to 1 km and employed to compute the monthly SMCI. The SMCI is defined as:

$$\mathrm{SMCI}=\frac{SM_i-SM_{\min}}{SM_{\max}-SM_{\min}} \quad (2)$$

where $SM_{max}$ and $SM_{min}$ represent the historical maximum and minimum SM values at each specified time step during the study period, and $SM_i$ is the SM in the $i$ month.

$i$=Time step representing a specific month.

To capture the vegetation and thermal conditions associated with drought, we then calculate the VCI and TCI. The equations of VCI and TCI are as follows:

$$\mathrm{VCI}=\frac{NDVI_i-NDVI_{\min}}{NDVI_{\max}-NDVI_{\min}} \quad (3)$$

$$\mathrm{TCI}=\frac{LST_{\max}-LST_i}{LST_{\max}-LST_{\min}} \quad (4)$$

where $LST_{max}$($NDVI_{max}$) and $LST_{min}$($NDVI_{min}$) are the historical highest and lowest LST (NDVI) values at each specified time point throughout the study period, $LST_i$ and $NDVI_i$ represent the LST and NDVI in the $i$ month (Kogan 1995a; Liu and Kogan 2007), $i$ is a time step representing a specific month.

### 2.4. Standardized precipitation evapotranspiration index

Referring to Ren *et al.* (2008), the 1-month SPI captures short-term conditions and is closely associated with meteorological drought. The 3-month SPI provides insights into soil moisture conditions at the beginning of the growing season, while the 6-month SPI may correlate with unusual river flows and reservoir levels. The 9-month SPI is generally a strong indicator of significant impacts on agriculture due to dryness. The 12-month SPI can reflect precipitation changes over a year and is suitable for identifying and analyzing regional climate trends and the consequences of climate change. In terms of agricultural drought, the SPI-12 can be used to characterize the consequences for agricultural output of crops that rely on multi-year water resource accumulation. Therefore, in this study, the SPEI, a commonly used *in-situ* drought measure, was calculated for 1-, 3-, 6-, 9-, and 12-month time scales using the aforementioned data. The SPI, calculated from historical precipitation data at various time scales, is used to monitor drought conditions associated with different water resources (McKee *et al.* 1993; Hayes *et al.* 1999). The SPEI, which extends the SPI, includes both potential evapotranspiration (PET) and precipitation to evaluate drought conditions. This integration enables the SPEI to factor in the impact of rising temperatures on water requirements, making it more flexible across various time scales compared to the SPI (Vicente-Serrano *et al.* 2010).

Precipitation and evapotranspiration are the primary factors influencing climate dryness and wetness. By incorporating both precipitation and PET, the SPEI can assess variations in dryness and wetness over different time scales. In this study, the SPEI was calculated for various time scales (1, 3, 6, 9, and 12 months) using the Thornthwaite method to calculate PET and precipitation data from 13 meteorological stations across Heilongjiang Province from 1986 to 2021. PET was calculated using the Thornthwaite method as follows:

$$PET=\begin{cases}0 & T<0\\ 16\left(\frac{N}{12}\right)\left(\frac{NDM}{30}\right)\left(\frac{10M}{1}\right)^m & 0\le T<26.5\\ -415.85+32.24T-0.43T^2 & T\ge 26.5\end{cases} \quad (5)$$

where $T$, $N$, and $NDM$ are the monthly mean temperature, maximum sunshine hours per day, and number of days per month.

Calculating the SPEI involves the following steps:

(1) Calculation of climatic water balance:

$$D_i=P_i-PET_i \quad (6)$$

where $D_i$ represents the climatic water balance for a given time step $i$, $P_i$ represents the precipitation at time step $i$, and $PET_i$ represents the potential evapotranspiration at time step $i$. Here, $i$ denotes the specific month or time step in the calculation period.

(2) Calculating cumulative sequences of climatic water balance at different time scales:

$$D_n^k=\sum_{i=0}^{k-1}(P_{n-1}-PET_{n-1}),\ n\ge k \quad (7)$$

where $k$ represents the selected timescale (e.g., 1, 3, 6, 9, or 12 months), and $n$ denotes the total number of time steps used in the computation.

(3) Fitting the data sequence using the log-logistic probability density function:

$$f(x)=\frac{\beta}{\alpha}\left(\frac{X-\gamma}{\alpha}\right)^{\beta-1}\left[1+\left(\frac{X-\gamma}{\alpha}\right)^{\beta}\right]^{-2}$$
$$F(x)=\left[1+\left(\frac{X-\gamma}{\alpha}\right)^{\beta}\right]^{-1} \quad (8)$$

where $\alpha$ is the time scale coefficient, $\beta$ is the shape coefficient, $\gamma$ is the origin parameter, and $F(x)$ is the cumulative probability for a given time scale.

(4) Obtaining the corresponding SPEI time series:

$$SPEI=W-\frac{C_0+C_1W+C_2W^2}{1+d_1W+d_2W^2+d_3W^3} \quad (9)$$

where $W$ is a parameter, its value is $\sqrt{-2\ln(p)}$, where $p$ is the probability of exceeding the determined moisture surplus or deficit. When $p \leq 0.5$, $p=1-F(x)$; when $p>0.5$, $p=1-p$, and the sign of SPEI is reversed. Other constants in the equation are: $C_0$= 2.515517, $C_1$=0.802853, $C_2$=0.010328, $d_1$=1.432788, $d_2$=0.189269, and $d_3$=0.001300 (Vicente-Serrano *et al.* 2010).

### 2.5. Computation of multivariable linear regression

Many problems that can be addressed using nonlinear and polynomial regressions can also be solved with multiple linear regression. Consequently, multiple linear regression is widely used across various fields (Montgomery *et al.* 2021). Multivariable linear regression refers to the influence of multiple factors on one result and has $n$ independent variables and a dependent variable $Y$. The formula is approximated by:

$$Y=\beta_0+\beta_1X_1+\beta_2X_2+...+\beta_jX_j+\varepsilon,\ j=1,2,3,...n \quad (10)$$

where $\varepsilon$ represents random experimental error, $\beta_0$ is the constant term, $\beta_1$, ...,$\beta_j$ are the coefficients for $X_1$, $X_2$ ..., $X_j$. When $\beta_j$($j$=1,2,3, ...$n$) is greater than 0, a higher value of $\beta_j$($j$=1,2,3, ...$n$) indicates a greater influence of $X_j$($j$=1,2,3, ...$n$) to Y. In this study, the variables Y were SPEIs, while $X_1$, $X_2$..., $X_j$ represented PCI, SMCI, TCI, and VCI.

Multivariable linear regression was employed to integrate multiple drought-related variables, including precipitation, soil moisture, temperature, and vegetation indices, into a composite drought index. The regression model was trained using historical drought data with the standardized precipitation. The selection of predictor variables was based on their correlation with SPEI, ensuring that only statistically significant factors were included in the regression model. The regression coefficients were determined using the least squares method, minimizing the residual sum of squares to optimize the fit of the model.

The MCDI is calculated by integrating precipitation, soil moisture, vegetation, and temperature data using a multivariable linear regression model. MCDI values for different timescales (1, 3, 6, 9, and 12 months) were calculated by aggregating the weighted contributions of precipitation, soil moisture, and temperature data over the specified period, with each timescale providing insight into short-term or long-term drought trends. Drought severity is classified into five levels: extreme, severe, moderate, mild, and slight drought, with MCDI values greater than 0 indicating no drought or wet conditions. The MCDI was divided into five levels: –0.5<MCDI<0 (slight drought), –1.0<MCDI<–0.5 (mild drought), –1.5<MCDI<–1.0 (moderate drought), –2.0<MCDI<–1.5 (severe drought) and MCDI<–2.0 (extreme drought).

The monthly MCDI trends at the pixel scale in Heilongjiang Province from 2000 to 2021 were analyzed based on trend analysis methods. Based on the magnitude of the trend values, they are divided into five categories: significantly decreasing (Slope<0, $P$<0.05), slightly decreasing (Slope<0, $P$>0.05), stable (Slope=0), slightly increasing (Slope>0, $P$>0.05), and significantly increasing (Slope>0, $P$<0.05). The overall approach is depicted in Fig. 2.

## 3. Results

### 3.1. Correlations between single remote sensing drought indices and *in-situ* drought indices

Values from remote sensing indices were obtained according to the positions of *in-situ* meteorological stations throughout the chosen time frame (Zuo *et al.* 2019). To assess the importance of each remote sensing index in drought monitoring, the correlation between each remote sensing index and the *in-situ* drought index (SPEI) within the study area was analyzed.

To construct MCDI, four widely used remote sensing-based drought indices were selected: PCI, SMCI, VCI,

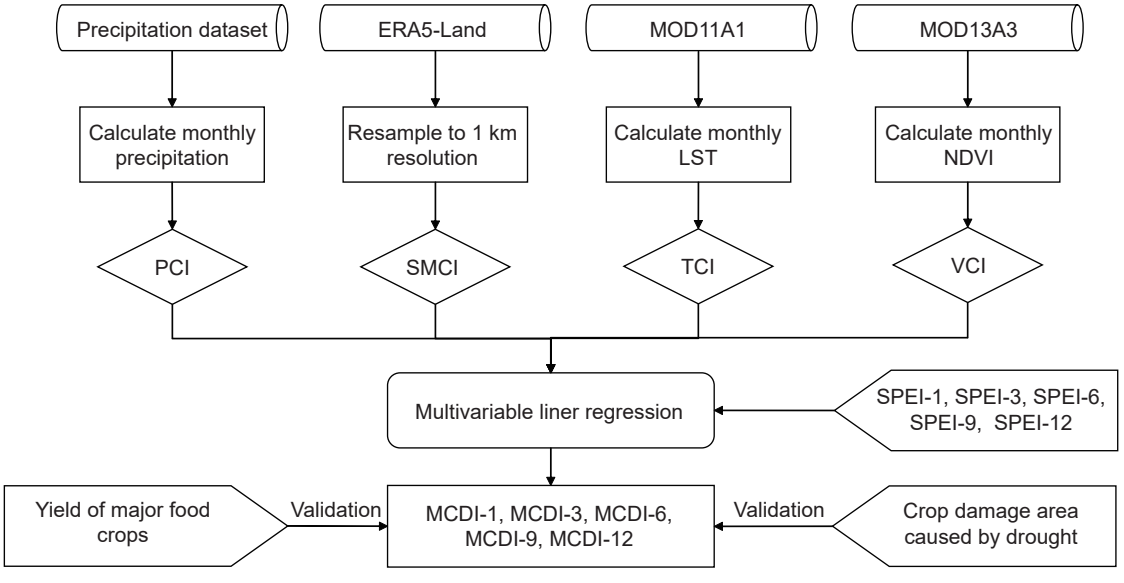



**Fig. 2 The flowchart of multi-source composite drought indices (MCDIs) establishment based on the multivariable linear regression method.**

and TCI. These indices were chosen based on their ability to capture different aspects of drought, ensuring a comprehensive representation of drought conditions across meteorological, soil moisture, vegetation, and thermal domains. The selection of these indices is supported by previous studies demonstrating their effectiveness in drought assessment across various regions. By integrating these indices, the MCDI captures multiple dimensions of drought impacts, improving its robustness and applicability.

The performance of MCDI was validated by comparing its values with SPEI and historical agricultural drought impact data, such as crop yield reductions and affected crop areas.

Table 1 reveals that PCI has the highest correlation with SPEI-1 ($r$=0.66), suggesting that PCI is the most effective at observing short-term drought versus other standalone remote sensing indices. Additionally, the correlation decreases as the SPEI time scale increases. SMCI exhibits the highest correlation with SPEI-6 among the single indices, reflecting its strong connection to soil moisture and its reliability in monitoring vegetation droughts. Similarly, TCI has the highest correlation with SPEI-1, the trend of change is similar to that of PCI. VCI shows a lower correlation with SPEIs than other indices, though VCI shows a higher correlation with SPEI-9 than with other SPEIs, suggesting that the drought information captured by VCI lags behind that captured by SMCI.

**Table 1 Correlation coefficients between single remote sensing drought indices and different time scales *in-situ* indices SPEI[1)]**

| | SPEI-1 | SPEI-3 | SPEI-6 | SPEI-9 | SPEI-12 |
|---|---|---|---|---|---|
| PCI ($n$=455) | 0.66 | 0.47 | 0.40 | 0.20 | 0.11 |
| SMCI ($n$=455) | 0.21 | 0.27 | 0.29 | 0.17 | 0.23 |
| TCI ($n$=455) | 0.37 | 0.36 | 0.26 | 0.25 | 0.27 |
| VCI ($n$=455) | 0.11 | 0.16 | 0.15 | 0.20 | 0.25 |

[1)] SPEI, standardized precipitation evapotranspiration index; PCI, precipitation condition index; SMCI, soil moisture condition index; TCI, temperature condition index; VCI, vegetation condition index. All $P$-values were less than 0.01. $n$ represents the total number of data points, calculated based on records from 13 meteorological stations during March–September in 2017–2021.

**Table 2 The coefficient, $P$-values of single remote sensing indices obtained by multivariable linear regression method[1)]**

| | | SPEI-1 | SPEI-3 | SPEI-6 | SPEI-9 | SPEI-12 |
|---|---|---|---|---|---|---|
| PCI | Coeff. | 3.860 | 2.876 | 2.434 | 1.164 | 0.632 |
| | $P$-value | 0.000 | 0.000 | 0.000 | 0.000 | 0.023 |
| SMCI | Coeff. | 3.080 | 3.995 | 4.342 | 2.539 | 3.302 |
| | $P$-value | 0.000 | 0.000 | 0.000 | 0.000 | 0.000 |
| TCI | Coeff. | 0.464 | 0.496 | 0.348 | 0.344 | 1.030 |
| | $P$-value | 0.000 | 0.035 | 0.000 | 0.000 | 0.000 |
| VCI | Coeff. | 0.018 | 0.172 | 0.216 | 0.372 | 1.189 |
| | $P$-value | 0.038 | 0.049 | 0.025 | 0.000 | 0.000 |

[1)] PCI, precipitation condition index; SMCI, soil moisture condition index; TCI, temperature condition index; VCI, vegetation condition index; SPEI, standardized precipitation evapotranspiration index.

## 3.2. Establishment of composite drought indices

Table 2 presents the coefficients of the variables obtained through multiple linear regression, along with their corresponding significance levels. All $P$-values of the coefficients are below 0.05, indicating statistical significance. This suggests that all four selected factors have varying degrees of influence on drought. Drought occurrence largely depends on precipitation and soil moisture, with precipitation having a direct impact on soil moisture levels. Additionally, LST influences the loss of soil moisture through evaporation, while vegetation also plays a role in drought conditions (Holzman *et al.* 2014; Wang *et al.* 2021).

Fig. 3 compares the maximum correlation between single remote sensing indices and SPEIs with the correlation between composite indices and SPEIs. The composite index shows a correlation of 0.03 to 0.12 higher than the single index. While each single index provides distinct information, composite indices integrate data from multiple single indices. The superior performance of MCDIs over individual indices suggests that MCDIs can better explain drought across different timescales and are more effective in monitoring drought than single remote sensing indices.

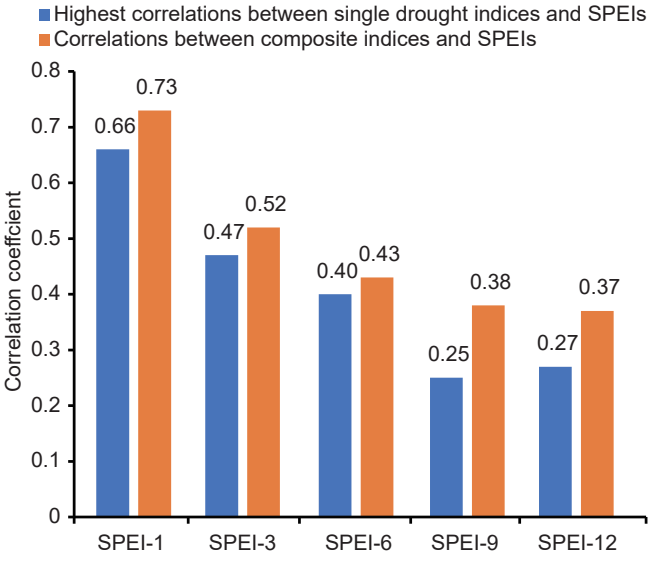



**Fig. 3 Comparison of the maximum correlation between single remote sensing indices and correlations between multi-source composite drought indices (MCDIs) and standardized precipitation evapotranspiration index (SPEIs).**

## 3.3. Comparisons of MCDIs with crop damage area and grain yield

The significant impact of shorter-scale droughts (3, 6, 9, and 12 months) might be reflected in agricultural yields (Hayes *et al.* 1999). We combined the crop damage area caused by drought in Heilongjiang Province, as reported in the *China Water and Drought Disaster Bulletin*, with the corn, rice, and total crop production data from the *Heilongjiang Statistical Yearbook* to study the drought behavior of the MCDI.

Fig. 4 shows the changes in crop damage area caused by drought in Heilongjiang Province over the 35 years from 1986 to 2021, as well as the corresponding MCDI-3, MCDI-6, MCDI-9, and MCDI-12. As the time scale increases, the $r$ value also increases. It indicates that the correlation between MCDI and the crop damage area becomes stronger over longer time scales. The regression models for MCDI-6, MCDI-9, and MCDI-12 are statistically significant ($P$<0.05),

whereas the model for MCDI-3 is not ($P$>0.05). This analysis demonstrates that MCDI on long-time scales has more significant effects on crops. Among them, MCDI-9 and MCDI-12 have the highest correlation with agricultural drought.

However, it is observed that MCDI does not perform well in certain years, such as 2016, 2010, and 1995–1996. Several factors may contribute to these discrepancies. In 2016, sudden short-term precipitation events likely mitigated drought effects on crops, making the impact less pronounced in the statistical data despite dry conditions being detected. Similarly, in 2010, rapid shifts between wet and dry conditions may have influenced MCDI calculations, leading to inconsistencies in correlation with crop damage. For 1995–1996, changes in agricultural practices, such as irrigation expansion and crop variety adjustments, may have reduced the observed drought impact, making it less detectable by MCDI despite meteorological drought conditions. These factors highlight the complexity of drought impacts and the need to consider additional variables, such as irrigation and soil water retention capacity, in future improvements of the MCDI.

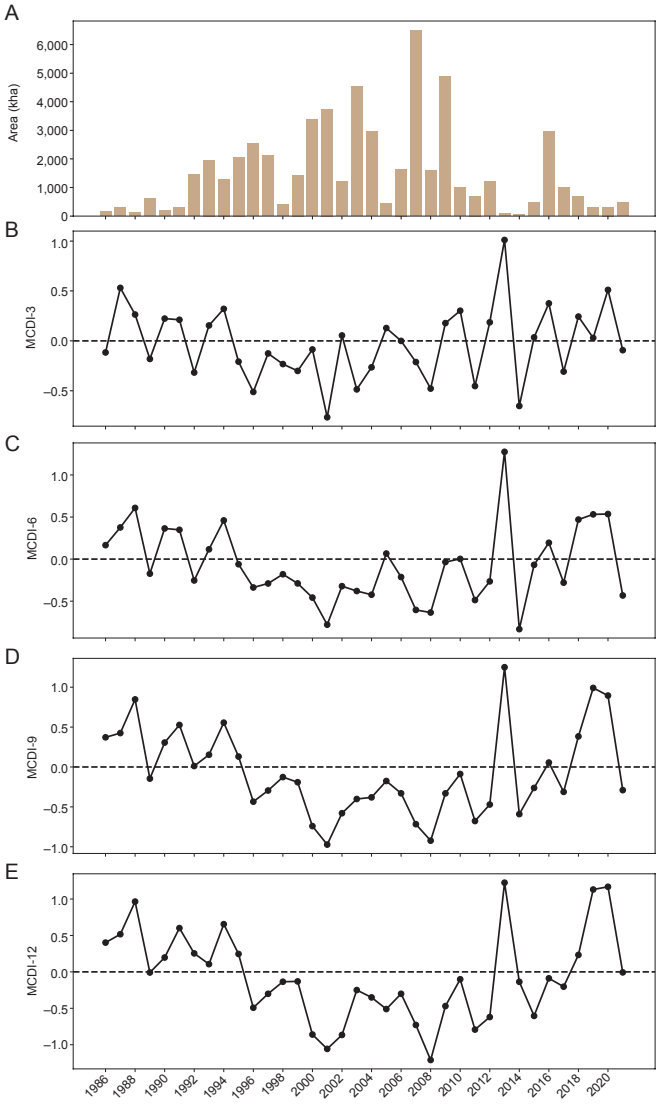



**Fig. 4 Time series of the affected area of crops due to drought (A) and multi-source composite drought index (MCDI-3, -6, -9, -12) (B–E) in Heilongjiang Province, China from 1986 to 2021.**

Fig. 5 shows the temporal variation of MCDI-3, MCDI-6, MCDI-9, and MCDI-12, along with the variation in corn, rice, and total crop production from 2000 to 2021 at the regional scale. Rice and maize were selected due to their economic importance in Heilongjiang Province and their high sensitivity to drought conditions during the growing season. As the time span increases, the correlation between MCDI and corn production (CP), rice production (RP), and total crop production (TP) gradually strengthens. To make it comparable with MCDIs, we standardized CP, RP and TP; then, MCDIs values were averaged over the years. Specifically, the correlation between TP and MCDI is slightly higher than that of CP and RP, as TP includes multiple crops, while corn and rice are only a part of it. Due to corn being more susceptible to drought during its growing season, the correlation between MCDI and CP is slightly higher than between MCDI and RP. The correlation between MCDI-12 and various crop yields is most significant, with correlation coefficients of 0.561 (TP), 0.553 (CP), and 0.527 (RP). This indicates that longer time spans of drought indices more accurately reflect changes in crop yields.

### 3.4. Spatial patterns of MCDIs

MCDI-9 and MCDI-12 were selected for analysis due to their strong correlation with agricultural drought indicators, particularly crop damage area and yield reductions. Previous studies have demonstrated that longer timescale drought indices provide a more stable representation of drought impacts on agricultural production, as they account for cumulative moisture deficits over extended periods. Thus, MCDI-9 and MCDI-12 are considered more suitable for assessing the long-term effects of drought on crop growth and yield. The spatial distribution of MCDI-9 across different months during the crop sowing season (March to September) in Heilongjiang Province in 2021 (a typical wet year) is shown in Fig. 6-A. In the study period, the central and southeastern regions of Heilongjiang Province experienced varying degrees of drought. Early in the season, drought conditions were mostly mild. However, as the season progressed, the extent and severity of the drought increased, peaking in August with extensive areas experiencing extreme drought. By September, the situation was slightly alleviated, but severe drought persisted in the southern regions, and mild to moderate drought continued in localized areas of the central and southeastern regions.

Fig. 6-B shows the spatial distribution of MCDI-12 during the planting season in Heilongjiang Province in 2021. From March to September, both the extent and severity of drought conditions varied. In the early period (March to June), drought was primarily concentrated in the northern regions. However, from July to September, the drought-affected areas gradually expanded towards the central and southeastern regions. Throughout most of the planting season, drought conditions were relatively mild. However, in September, drought in the southeastern region significantly intensified, reaching moderate to severe levels. Drought initially emerged in the northern and central regions and then

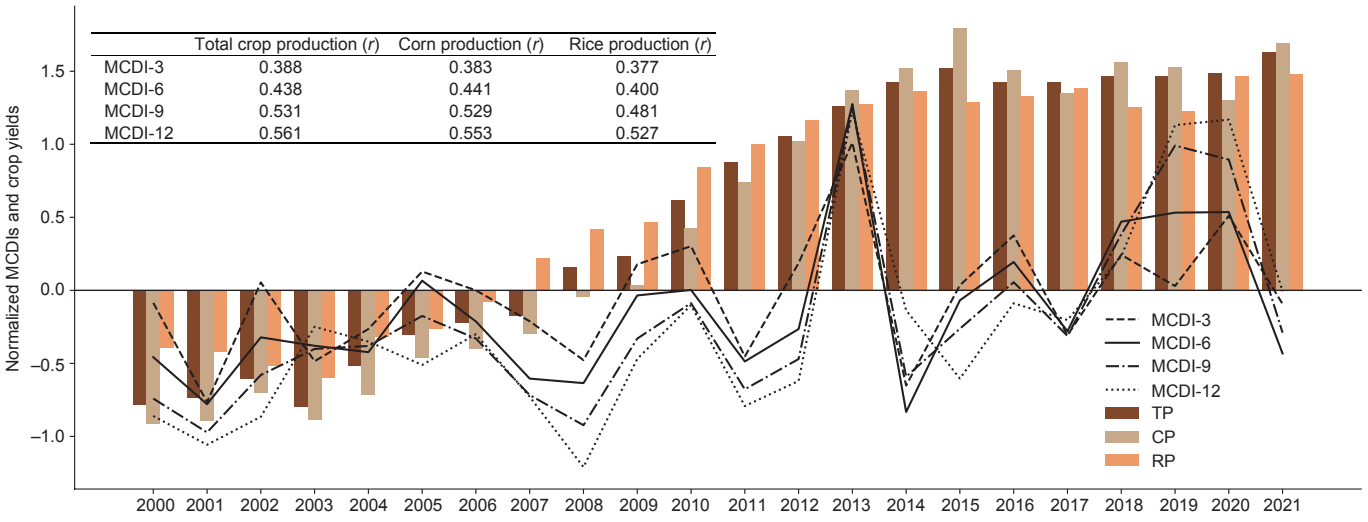



**Fig. 5 Yearly averaged multi-source composite drought indices (MCDIs) at 3- to 12-month time scales with crop production from 2000 to 2021.** TP, total crop production; CP, corn production; RP, rice production. The table shows the correlation between MCDIs and the overall yield of each crop over 20 years.

spread to the southeast by the end of the planting season (September), indicating differing drought risks across various regions at different times.

The main difference between the MCDI-9 and MCDI-12 is their time scales, which influence their sensitivity to climate anomalies and response speed. MCDI-9 is more effective for monitoring mid-term drought fluctuations, while MCDI-12 better reflects long-term drought trends.

Fig. 7-A shows the spatial distribution of MCDI-9 during the planting season of Heilongjiang Province in 2007, a typical drought year. Drought began to appear in the northern and central regions in March and gradually expanded to the southern regions. From April to June, the range and severity of the drought increased month by month, with the southern regions experiencing significant intensification of drought after June. As the planting season progressed, the cumulative effects of the drought became increasingly evident. Extreme drought began to appear from July to August, with many areas in the southern, central, and northern regions experiencing severe to extreme drought, and this condition persisted without significant relief until September.

MCDI-12 shows that in 2007, drought in Heilongjiang Province gradually expanded from the northern and central regions in early spring to the southern regions in summer, exhibiting significant seasonal variations. Early drought (March to May) was mainly concentrated in the northern and central regions, which are more prone to drought during the early spring. Later, drought (June to September) began to extend to the southern regions, with extreme drought occurring in the central and southern areas. The cumulative effects of the drought intensified throughout the planting season, reaching their peak in July and August, as shown in Fig. 7-B.

The spatial analysis of MCDI-9 and MCDI-12 in 2007 reveals a clear progression of drought severity, with conditions worsening from early spring to late summer. The results indicate that these indices effectively captured the drought event, aligning well with SPEI-based drought classification and reported agricultural losses. This consistency underscores the applicability of MCDI for monitoring severe drought events in Heilongjiang Province.

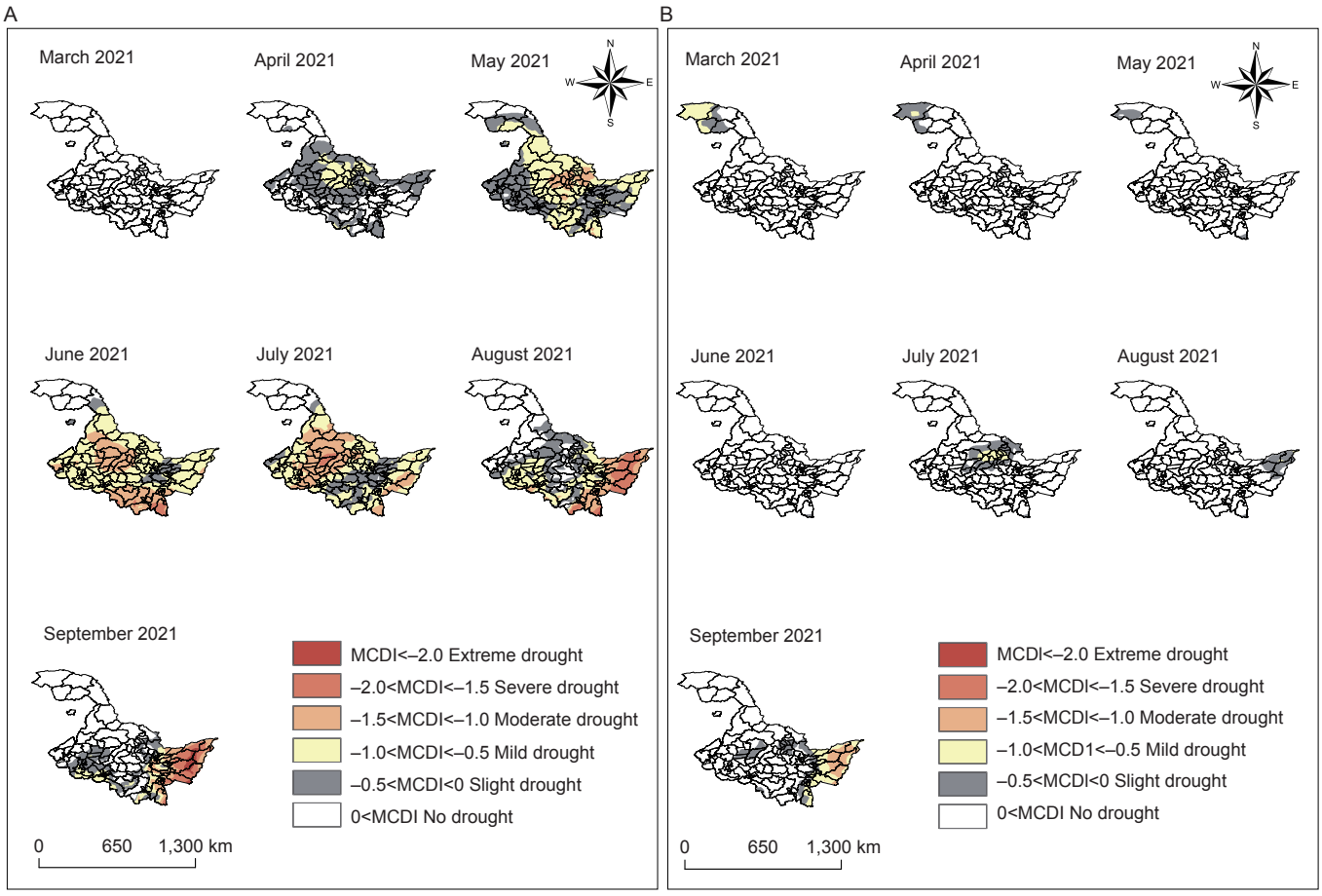
### 3.5. Interannual variation in MCDIs

The areas with significant increases in MCDI-12 are noticeably more extensive than those in MCDI-9, indicating a more pronounced wetting trend on a longer time scale. In contrast, the significantly decreased areas in MCDI-9 reflect a drought trend on a shorter time scale.

Tables 3 and 4 show the percentage of pixels with different variation trends for MCDI-9 and MCDI-12 each month. Overall, MCDI-9 indicates that the percentage of high-risk drought areas starts to increase in March, reaches its peak in April and May, begins to decrease in June, and drops to zero in September. On the other hand, MCDI-12 represents more of an interannual variation, with the high-risk percentage gradually decreasing from March to September, eventually reaching zero.

Fig. 8 shows the monthly variation trend of MCDI-9. On a shorter time scale, the northern and central regions exhibit a significant drought trend in the early period (March to May), while the central and western regions show a wetting trend in the later period (June to September). From March to May, the northern and central regions show a significant decrease, indicating a gradual drying trend, and the southern and eastern regions show a slight decreasing trend. From June to September, the areas with significant decreases gradually reduce, while the central and western regions show a slight increase, and parts of the southern and eastern regions also exhibit significant increases, indicating that these regions are gradually becoming wetter during this period.

Fig. 9 shows the monthly variation trend of MCDI-12. On a longer time scale, Heilongjiang Province shows a more significant wetting trend. The central and western regions gradually become wetter throughout the planting period, while the northern region experiences fewer significant changes.




审图号 : GS 京 (2025) 2497 号

**Fig. 6 Spatial distribution of drought monitored by multi-source composite drought index (MCDI-9) (A) and MCDI-12 (B) in the typical wet year (2021) from March to September.**

From March to September, areas with significant decreases are mostly limited to small parts of the northern and eastern regions. The central and southern regions exhibit a significant increasing trend throughout the planting period, particularly from July to September, indicating a gradual wetting trend over a longer time scale. Small parts of the northern and southern regions show a slight decreasing trend, while most of the central and western regions show a slight increase.

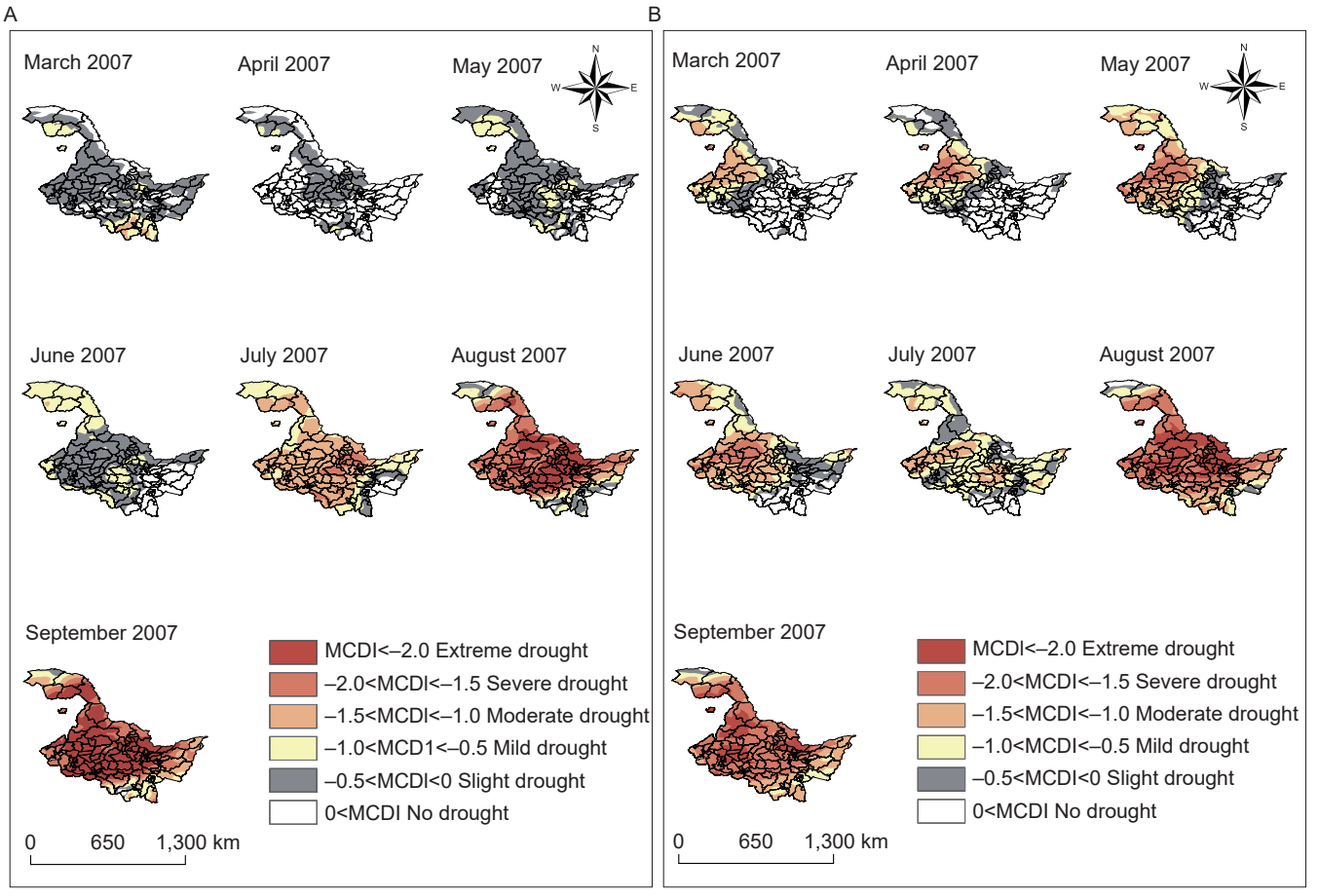
## 4. Discussion

The monsoon and geographical environment influence the spatiotemporal distribution of precipitation in Heilongjiang Province, leading to a very uneven pattern. This uneven distribution significantly impacts agriculture, as short-term droughts during critical growth periods have substantial effects. Thus, analyzing drought changes in this region has practical significance.

Heilongjiang Province exhibits pronounced interannual variability in its dry and wet periods, generally trending from drought to wetter conditions over time. This study highlighted that the change from dry to wet periods is staged and exhibits distinct trends. The annual variability is evident, which underscores the importance of understanding these patterns for effective agricultural planning and water resource management.

Spatially, variations in dry and wet conditions also exhibit prominent interannual characteristics. The spatial distribution maps of MCDI-9 and MCDI-12 for a typical wet year (2021) and a typical drought year (2007) reveal the regional impacts of drought. In 2007, drought conditions began in the northern and central regions in early spring and gradually expanded southwards, intensifying significantly by summer. The persistence of extreme drought conditions until September underscores the importance of early drought detection and management strategies. Heilongjiang Province's regional differentiation is primarily influenced by solar radiation and large-scale weather characteristics. However, the regional differences are not particularly pronounced (Liu *et al.* 2024).

In terms of agricultural drought, Heilongjiang Province exhibits strong seasonal characteristics. The analysis of MCDI-9 and MCDI-12 reveals that the spatio-temporal distribution of drought is relatively dispersed. Therefore, studying drought trends at the agricultural field scale is of significant importance. On a temporal scale, Figs. 8 and 9 show that Heilongjiang Province is generally trending towards more humid conditions. However, the risk of drought increases during the early spring, especially in April and May during the crop-growing season. Starting from July, as precipitation increases and soil water retention




审图号 : GS 京 (2025) 2497 号

**Fig. 7 Spatial distribution of drought monitored by multi-source composite drought index (MCDI-9) (A) and MCDI-12 (B) in the typical drought year (2007) from March to September.**

capacity improves, the drought risk begins to decrease. By September, the areas at risk of drought gradually diminish and eventually stabilize (Zhou *et al.* 2020).

In addition, the linear regression method used to construct the multi-source composite drought index (MCDI) in this study has been shown to be effective in integrating multiple drought-related variables. However, as noted in previous studies, nonlinear methods such as machine learning approaches could potentially capture more complex relationships between drought-related variables. Nonlinear models, such as Random Forest or Support Vector Machines, have been increasingly explored in drought monitoring due to their ability to handle large datasets and capture nonlinear interactions. While linear models offer simplicity and interpretability, nonlinear methods may provide more accurate predictions in some cases, especially in areas with highly variable climate patterns. Future research could explore hybrid approaches combining the strengths of both linear and nonlinear methods to optimize drought monitoring capabilities.

Moreover, the use of MCDI in Heilongjiang Province provides significant advantages for drought monitoring in the region. The combination of multiple remote sensing indices, such as vegetation condition and land surface temperature, with meteorological data allows for a more comprehensive assessment of drought conditions. Compared to traditional drought indices, MCDI provides a higher spatial resolution, enabling more detailed monitoring across different regions. Additionally, its multi-timescale analysis is particularly useful in capturing both short-term and long-term drought patterns, which is critical for agricultural management in the region.

However, it is important to acknowledge that factors such as irrigation practices, soil water retention capacity, and regional agricultural practices also play a significant role in influencing drought impacts on crops. For example, irrigation systems can mitigate the effects of meteorological drought, especially in areas with limited precipitation. Similarly, soil properties such as organic matter content and texture can significantly affect the soil's ability to retain moisture, thus influencing crop yields during drought periods. Regional agricultural practices, including crop selection and land management strategies, may further modify the vulnerability of crops to drought conditions. Incorporating these additional variables into future drought monitoring models could provide a more comprehensive and accurate assessment of drought impacts on agricultural productivity.

## 5. Conclusion

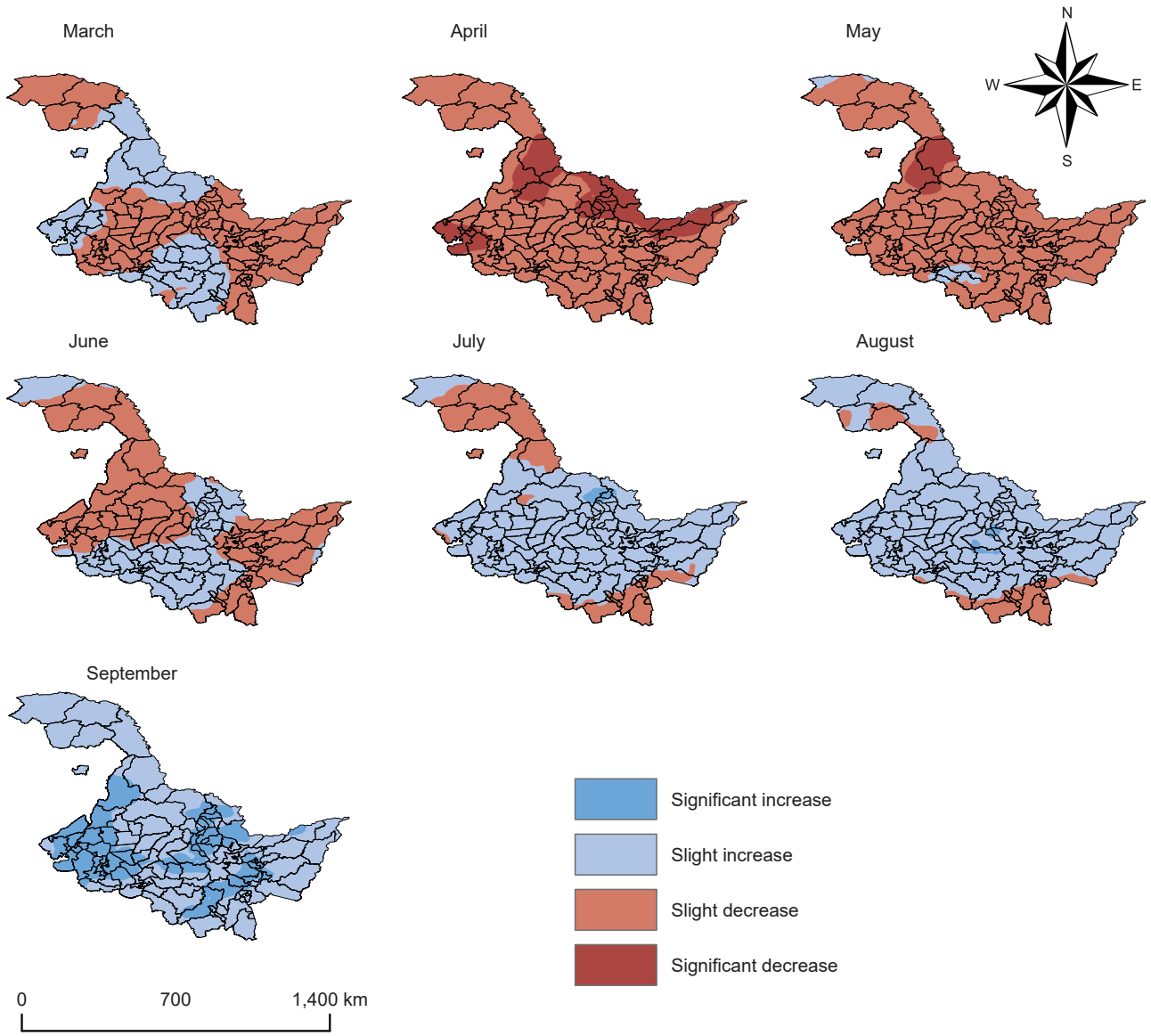
This study develops MCDI and analyzes the spatio-temporal

**Table 3 Percentage (%) of pixels with different variation trends for multi-source composite drought index (MCDI-9) from March to September**

| Type of trend | March | April | May | June | July | August | September |
|---|---|---|---|---|---|---|---|
| Significant decrease | 0.000 | 22.198 | 5.641 | 0.000 | 0.000 | 0.000 | 0.000 |
| Slight decrease | 61.926 | 77.802 | 91.434 | 65.336 | 23.967 | 11.557 | 0.000 |
| Stable | 0.000 | 0.000 | 0.000 | 0.000 | 0.000 | 0.000 | 0.000 |
| Slight increase | 38.074 | 0.000 | 2.925 | 34.664 | 74.917 | 87.467 | 68.905 |
| Significant increase | 0.000 | 0.000 | 0.000 | 0.000 | 1.116 | 0.976 | 31.095 |

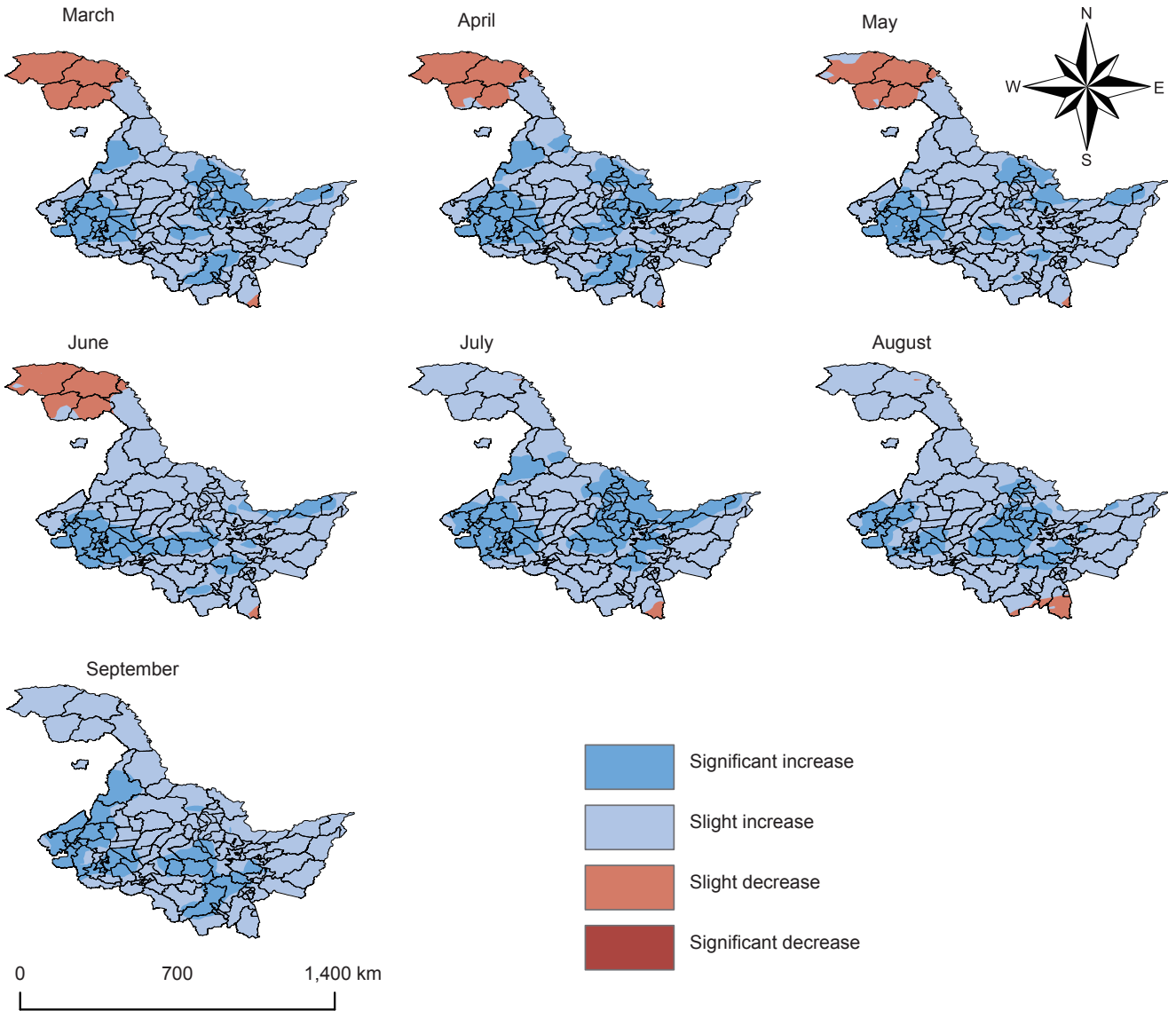
**Table 4 Percentage (%) of pixels with different variation trends for multi-source composite drought index (MCDI-12) from March to September**

| Type of trend | March | April | May | June | July | August | September |
|---|---|---|---|---|---|---|---|
| Significant decrease | 0.000 | 0.000 | 0.000 | 0.000 | 0.000 | 0.000 | 0.000 |
| Slight decrease | 12.784 | 11.713 | 11.519 | 11.988 | 0.607 | 1.669 | 0.000 |
| Stable | 0.000 | 0.000 | 0.000 | 0.000 | 0.000 | 0.000 | 0.000 |
| Slight increase | 62.138 | 57.511 | 70.988 | 69.101 | 65.962 | 77.258 | 75.280 |
| Significant increase | 25.078 | 30.776 | 17.493 | 18.911 | 33.431 | 21.073 | 24.720 |




审图号 : GS 京 (2025) 2497 号

**Fig. 8 Spatial distribution of monthly variation trend types of multi-source composite drought index (MCDI-9) in Heilongjiang Province, China.**




审图号 : GS 京 (2025) 2497 号

**Fig. 9 Spatial distribution of monthly variation trend types of multi-source composite drought index (MCDI-12) in Heilongjiang Province, China.**

drought characteristics in Heilongjiang Province during the crop-growing season. The following important conclusions were obtained:

(1) The MCDI effectively monitors drought by integrating multiple drought-related variables, overcoming limitations of single-index methods in spatial resolution, coverage, and update frequency. Compared to traditional indices like MDSI and NSPEI, MCDI provides a more comprehensive and flexible approach.

(2) The results indicate that MCDI-9 and MCDI-12 are more effective in capturing the regional impact of drought, especially in areas where drought tends to persist over multiple months.

(3) The comparison of MCDI-9 and MCDI-12 for a typical drought year and a typical wet year indicates that drought areas vary significantly by phase and region. Drought begins in the northern and central regions in early spring and gradually expands southward.

(4) Crop growth is severely affected by drought during the early part of the growing season. Early monitoring and timely interventions, such as irrigation and replanting, can mitigate yield losses.

## Acknowledgements

This work was supported by the National Key Research and Development Program of China (2022YFD2001105).

## Declaration of competing interest

The authors declare that they have no conflict of interest.

## Declaration of generative AI and AI-assisted technologies in the writing process

The authors declare that they did not use AI in the preparation and writing of this manuscript.

## References


Ahmed K, Shahid S, Chung E S, Wang X J, Harun S B. 2019. Climate change uncertainties in seasonal drought severity-area-frequency curves: Case of arid region of Pakistan. *Journal of Hydrology*, **570**, 473–485.

Bezdan J, Bezdan A, Blagojević B, Mesaroš M, Pejić B, Vranešević M, Pavić D, Nikolić-Đorić E. 2019. SPEI-based approach to agricultural drought monitoring in Vojvodina region. *Water*, **11**, 1481.

Bhardwaj J, Kuleshov Y, Chua Z W, Watkins A B, Choy S, Sun Q. 2022. Evaluating satellite soil moisture datasets for drought monitoring in Australia and the South-West Pacific. *Remote Sensing*, **14**, 3971.

Chen W Y, Xiao Q G, Sheng Y W. 1994. Application of the anomaly vegetation index to monitoring heavy drought in 1992. *Remote Sensing of Environment*, **9**, 106–112.

Dan W, Wei H, Shuwen Z, Kun B, Bao X, Yi W, Yue L. 2015. Processes and prediction of land use/land cover changes (LUCC) driven by farm construction: The case of Naoli River Basin in Sanjiang Plain. *Environmental Earth Sciences*, **73**, 4841–4851.

Du L, Tian Q, Yu T, Meng Q, Jancso T, Udvardy P, Huang Y. 2013. A comprehensive drought monitoring method integrating MODIS and TRMM data. *International Journal of Applied Earth Observation and Geoinformation*, **23**, 245–253.

El-Beltagy A, Madkour M J A, Security F. 2012. Impact of climate change on arid lands agriculture. *Journal of Arid Environments*, **1**, 1–12.

Ezenwaji E, NzoiwuC, Chima G. 2017. Analysis of precipitation concentration index (PCI) for Awka urban area, Nigeria. *Hydrology: Current Research*, **8**, 1–6.

Haile G G, Tang Q, Li W, Liu X, Zhang X. 2020. Drought: Progress in broadening its understanding. *Wiley Interdisciplinary Reviews Water*, **7**, e1407.

Hao C, Zhang J, Yao F. 2015. Combination of multi-sensor remote sensing data for drought monitoring over Southwest China. *International Journal of Applied Earth Observation and Geoinformation*, **35**, 270–283.

Hayes M J, Svoboda M D, Wiihite D A, Vanyarkho O V. 1999. Monitoring the 1996 drought using the standardized precipitation index. *Bulletin of the American Meteorological Society*, **80**, 429–438.

Holzman M E, Rivas R, Piccolo M C. 2014. Estimating soil moisture and the relationship with crop yield using surface temperature and vegetation index. *International Journal of Applied Earth Observation and Geoinformation*, **28**, 181–192.

Jiang Q, Li W, Fan Z, He X, Sun W, Chen S, Wen J, Gao J, Wang J. 2021. Evaluation of the ERA5 reanalysis precipitation dataset over Chinese Mainland. *Journal of Hydrology*, **595**, 125660.

Kahil M T, Dinar A, Albiac J. 2015. Modeling water scarcity and droughts for policy adaptation to climate change in arid and semiarid regions. *Journal of Hydrology*, **522**, 95–109.

Kogan F N. 1995a. Application of vegetation index and brightness temperature for drought detection. *Advances in Space Research*, **15**, 91–100.

Kogan F N. 1995b. Droughts of the late 1980s in the United States as derived from NOAA polar-orbiting satellite data. *Bulletin of the American Meteorological Society*, **76**, 655–668.

Kogan F N. 1997. Global drought watch from space. *International Journal of Remote Sensing*, **78**, 621–636.

Kogan F N. 2007. Remote sensing of weather impacts on vegetation in non-homogeneous areas. *International Journal of Remote Sensing*, **11**, 1405–1419.

Koutroulis A G. 2019. Dryland changes under different levels of global warming. *Science of the Total Environment*, **655**, 482–511.

Kustas W P, Mecikalski J R, Pimstein A, Wardlow B, Hain C, Anderson M C. 2011. Evaluation of drought indices based on thermal remote sensing of evapotranspiration over the continental United States. *Journal of Climate*, **24**, 2025–2044.

Kuwayama Y, Thompson A, Bernknopf R, Zaitchik B, Vail P. 2019. Estimating the impact of drought on agriculture using the US Drought Monitor. *American Journal of Agricultural Economics*, **101**, 193–210.

Li Y, Chang J, Gao X, Zhang L, Wang L, Ren C. 2024. A case study on the impacts of future climate change on soybean yield and countermeasures in Fujin city of Heilongjiang province, China. *Frontiers in Agronomy*, **6**, 1257830.

Liu W T, Kogan F N. 2007. Monitoring regional drought using the Vegetation Condition Index. *International Journal of Remote Sensing*, **17**, 2761–2782.

Liu X, Cao K, Li M. 2024. Assessing the impact of meteorological and agricultural drought on maize yields to optimize irrigation in Heilongjiang Province, China. *Journal of Cleaner Production*, **434**, 139897.

Liu Y, Hwang Y. 2015. Improving drought predictability in Arkansas using the ensemble PDSI forecast technique. *Stochastic Environmental Research Risk Assessment*, **29**, 79–91.

McKee T B, Doesken N J, Kleist J. 1993. The relationship of drought frequency and duration to time scales. In: *Proceedings of the 8th Conference on Applied Climatology*. pp. 179–184.

Meyer S J. 1992. Drought and natural resources management in the United States: Impacts and implications of the 1987–89 drought. *Great Plains Research*, **2**, 312.

Michael C, Charles H, James R, Hill J, Stefan S, Graham V M. 2018. *World Atlas of Desertification*. Publications Office of the European Union, Luxembourg. pp. 1–69.

Mishra A, Bruno E, Zilberman D. 2021. Compound natural and human disasters: Managing drought and COVID-19 to sustain global agriculture and food sectors. *Science of the Total Environment*, **754**, 142210.

Mishra A K, Singh V P. 2010. A review of drought concepts. *Journal of Hydrology*, **391**, 202–216.

Montgomery D C, Peck E A, Vining G G. 2021. *Introduction to Linear Regression Analysis*. John Wiley Sons, Hoboken, New Jersey.

Mukhawana M B, Kanyerere T, Kahler D. 2023. Review of *in-situ* and remote sensing-based indices and their applicability for integrated drought monitoring in South Africa. *Water*, **15**, 240.

Palmer W C. 1965. *Meteorological Drought*. *US* (Research Paper No. 45). Retrieved from US Department of Commerce, Weather Bureau. Washington, D.C.

Peng S, Ding Y, Wen Z, Chen Y, Cao Y, Ren J. 2017. Spatiotemporal change and trend analysis of potential evapotranspiration over the Loess Plateau of China during 2011–2100. *Agricultural and Forest Meteorology*, **233**, 183–194.

Prăvălie R. 2016. Drylands extent and environmental issues. A global approach. *Earth-Science Reviews*, **161**, 259–278.

Ren G, Zhou Y, Chu Z, Zhou J, Zhang A, Guo J, Liu X. 2008. Urbanization effects on observed surface air temperature trends in North China. *Journal of Climate*, **21**, 1333–1348.

Rhee J, Im J, Carbone G J. 2010. Monitoring agricultural drought for arid and humid regions using multi-sensor remote sensing data. *Remote Sensing of Environment*, **114**, 2875–2887.

Sabater J M. 2019. ERA5-Land monthly averaged data from 1950 to present. Copernicus climate change service (C3S) climate data store (CDS) [DS]. [2023-11-23]. https://cds.climate.copernicus.eu/datasets/reanalysis-era5-land-monthly-means?tab=overview

Saha A, Pal S C, Chowdhuri I, Roy P, Chakrabortty R, Shit M. 2023. Vulnerability assessment of drought in India: Insights from meteorological, hydrological, agricultural and socio-economic perspectives. *Gondwana Research*, **123**, 68–88.

Souza A G S S, Neto A R, de Souza L L. 2021. Soil moisture-based index for agricultural drought assessment: SMADI application in Pernambuco State-Brazil. *Remote Sensing of Environment*, **252**, 112124.

Sun P, Ma Z, Zhang Q, Singh V P, Xu C Y. 2022. Modified drought severity index: Model improvement and its application in drought monitoring in China. *Journal of Hydrology*, **612**, 128097.

Thornthwaite C W. 1955. *The Water Balance*. Laboratory of Climatology, Publications in Climatology, New Jersey.

Vicente-Serrano S M, Beguería S, Gimeno L, Eklundh L, Giuliani G, Weston D, El Kenawy A, López-Moreno J I, Nieto R, Ayenew T. 2012. Challenges for drought mitigation in Africa: The potential use of geospatial data and drought information systems. *Applied Geography*, **34**, 471–486.

Vicente-Serrano S M, Beguería S, López-Moreno J I. 2010. A multiscalar drought index sensitive to global warming: The standardized precipitation evapotranspiration index. *Journal of Climate*, **23**, 1696–1718.

Vicente-Serrano S M, Quiring S M, Peña-Gallardo M, Yuan S, Domínguez-Castro F. 2020. A review of environmental droughts: Increased risk under global warming? *Earth-Science Reviews*, **201**, 102953.

Vogt J V, Somma F. 2013. *Drought and Drought Mitigation in Europe*. Vol. 14. Springer Science Business Media, Berlin, Germany.

Wagner W, Lemoine G, Rott H. 1999. A method for estimating soil moisture from ERS scatterometer and soil data. *Remote Sensing of Environment*, **70**, 191–207.
Wang H, Chen Y, Pan Y, Li W. 2015. Spatial and temporal variability of drought in the arid region of China and its relationships to teleconnection indices. *Journal of Hydrology*, **523**, 283–296.
Wang Y, Fu B, Liu Y, Li Y, Feng X, Wang S. 2021. Response of vegetation to drought in the Tibetan Plateau: Elevation differentiation and the dominant factors. *Agricultural and Forest Meteorology*, **306**, 108468.
Waseem M, Ajmal M, Kim T W. 2015. Development of a new composite drought index for multivariate drought assessment. *Journal of Hydrology*, **527**, 30–37.
Wilhite D A, Glantz M H. 1985. Understanding: The drought phenomenon: The role of definitions. *Water International*, **10**, 111–120.
Willmott C J, Feddema J J. 1992. A more rational climatic moisture index. *Geographical Review*, **44**, 84–88.
Wu J, Liu Z, Yao H, Chen X, Chen X, Zheng Y, He Y. 2018. Impacts of reservoir operations on multi-scale correlations between hydrological drought and meteorological drought. *Journal of Hydrology*, **563**, 726–736.
Xu P, Zhou T, Zhao X, Luo H, Gao S, Li Z, Cao L. 2018. Diverse responses of different structured forest to drought in Southwest China through remotely sensed data. *International Journal of Applied Earth Observation and Geoinformation*, **69**, 217–225.
Zargar A, Sadiq R, Naser B, Khan F. 2011. A review of drought indices. *Environmental Reviews*, **19**, 333–349.
Zhang A, Jia J. 2013. Monitoring meteorological drought in semiarid regions using multi-sensor microwave remote sensing data. *Remote Sensing of Environment*, **134**, 12–23.
Zhang X, Chen N, Li J, Chen Z, Niyogi D. 2017. Multi-sensor integrated framework and index for agricultural drought monitoring. *Remote Sensing of Environment*, **188**, 141–163.
Zhao H, Gao G, An W, Zou X, Li H, Hou M. 2017. Timescale differences between SC-PDSI and SPEI for drought monitoring in China. *Physics and Chemistry of the Earth*, *Parts A/B/C*, **102**, 48–58.
Zhou M, Liu X, Meng Q, Zeng X, Zhang J, Li D, Wang J, Du W, Ma X. 2019. Additional application of aluminum sulfate with different fertilizers ameliorates saline-sodic soil of Songnen Plain in Northeast China. *Journal of Soils Sediments*, **19**, 3521–3533.
Zhou Z, Shi H, Fu Q, Li T, Gan T Y, Liu S. 2020. Assessing spatiotemporal characteristics of drought and its effects on climate-induced yield of maize in Northeast China. *Journal of Hydrology*, **588**, 125097.
Zia R, Nawaz M S, Siddique M J, Hakim S, Imran A. 2021. Plant survival under drought stress: Implications, adaptive responses, and integrated rhizosphere management strategy for stress mitigation. *Microbiological Research*, **242**, 126626.
Zuo D, Cai S, Xu Z, Peng D, Kan G, Sun W, Pang B, Yang H. 2019. Assessment of meteorological and agricultural droughts using *in-situ* observations and remote sensing data. *Agricultural Water Management*, **222**, 125–138.

Executive Editor-in-Chief Jinshui Wu
Managing Editor Lujuan Sun